

## On the freezing behavior and diffusion of water in proximity to single-supported zwitterionic and anionic bilayer lipid membranes

This content has been downloaded from IOPscience. Please scroll down to see the full text.

2014 EPL 107 28008

(<http://iopscience.iop.org/0295-5075/107/2/28008>)

View [the table of contents for this issue](#), or go to the [journal homepage](#) for more

Download details:

IP Address: 129.6.122.135

This content was downloaded on 06/08/2014 at 14:11

Please note that [terms and conditions apply](#).

# On the freezing behavior and diffusion of water in proximity to single-supported zwitterionic and anionic bilayer lipid membranes

A. MISKOWIEC<sup>1</sup>, Z. N. BUCK<sup>1</sup>, M. C. BROWN<sup>2</sup>, H. KAISER<sup>1</sup>, F. Y. HANSEN<sup>3</sup>, G. M. KING<sup>1</sup>, H. TAUB<sup>1(a)</sup>, R. JIJI<sup>2</sup>, J. W. COOLEY<sup>2</sup>, M. TYAGI<sup>4,5</sup>, S. O. DIALLO<sup>6</sup>, E. MAMONTOV<sup>6</sup> and K. W. HERWIG<sup>6</sup>

<sup>1</sup> *Department of Physics and Astronomy and University of Missouri Research Reactor, University of Missouri Columbia, MO 65211, USA*

<sup>2</sup> *Department of Chemistry, University of Missouri - Columbia, MO 65211, USA*

<sup>3</sup> *Department of Chemistry, Technical University of Denmark, IK 207 DTU DK-2800 Lyngby, Denmark*

<sup>4</sup> *Center for Neutron Research, National Institute of Standards and Technology Gaithersburg, MD 20899-6102, USA*

<sup>5</sup> *Department of Materials Science and Engineering, University of Maryland - College Park, MD 20742, USA*

<sup>6</sup> *Spallation Neutron Source, Oak Ridge National Laboratory - Oak Ridge, TN 37831, USA*

received 31 May 2014; accepted in final form 1 July 2014

published online 22 July 2014

PACS 87.16.D- – Membranes, bilayers, and vesicles

PACS 78.70.Nx – Neutron inelastic scattering

PACS 87.16.dj – Dynamics and fluctuations

**Abstract** – We compare the freezing/melting behavior of water hydrating single-supported bilayers of a zwitterionic lipid DMPC with that of an anionic lipid DMPG. For both membranes, the temperature dependence of the elastically scattered neutron intensity indicates distinct water types undergoing translational diffusion: bulk-like water probably located above the membrane and two types of confined water closer to the lipid head groups. The membranes differ in the greater width  $\Delta T$  of the water freezing transition near the anionic DMPG bilayer ( $\Delta T \sim 70$  K) compared to zwitterionic DMPC ( $\Delta T \sim 20$  K) as well as in the abruptness of the freezing/melting transitions of the bulk-like water.

editor's choice

Copyright © EPLA, 2014

The structure and dynamics of the water hydrating lipid membranes and its effect on the functioning of membrane-embedded proteins involve some of the most fundamental issues in biological physics today. Although the dynamics of membrane-associated water has been studied for over four decades by nuclear magnetic resonance (NMR) [1–6] and quasielastic neutron scattering (QENS) techniques [4,7–11], previous investigations have primarily used multilamellar membrane systems. Unfortunately, their large size and complexity renders modeling of their water analytically or by computer simulations virtually impossible.

Recently, we have used high-energy-resolution QENS measurements to elucidate the diffusion of water molecules

in proximity to single bilayer membranes supported on a silicon-oxide ( $\text{SiO}_2$ ) substrate (see sketch in fig. 1(a)). For this purpose, we investigated DMPC membranes (1,2-Dimyristoyl-*sn*-glycero-3-phosphocholine) that have charge neutral (zwitterionic) lipid head groups. The relative simplicity of these single-supported membranes has allowed us to identify three different water types based on their diffusive motion: bulk-like water probably located above the membrane, confined water closer to the lipid head groups, and bound water molecules that move on the same time scale as H atoms in the lipids [12]. The bulk-like water is shown in fig. 1(a) whereas the confined and bound water types are not labeled. Analysis of the relative intensity of the spectral component contributed by the more slowly diffusing bound water allowed us to estimate that 7–10 water molecules on average were tightly bound

<sup>(a)</sup>E-mail: taubh@missouri.edu (corresponding author)

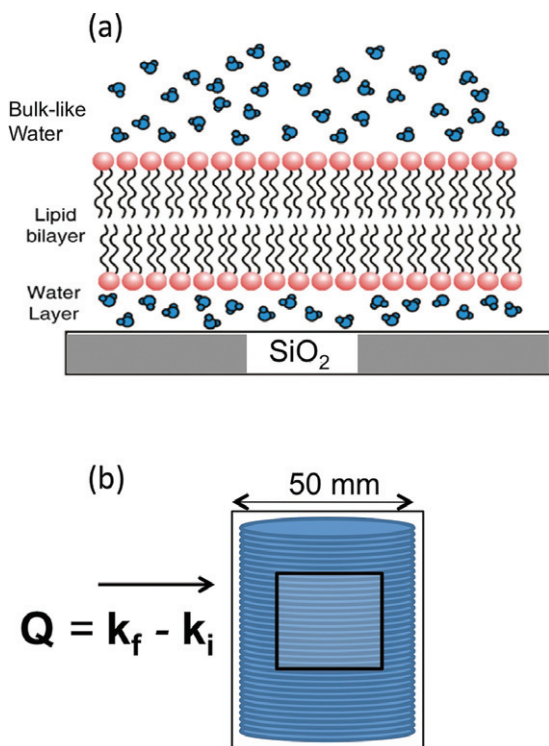


Fig. 1: (Color online) (a) Sketch of a hydrated single-supported bilayer membrane adapted from ref. [14]. The water layer between the lipid head groups in the lower leaflet and the  $\text{SiO}_2$  surface is believed to be too thin to contribute significantly to the QENS (see ref. [18]). (b) Schematic diagram of the neutron scattering sample consisting of a stack of Si(100) wafers, indicating the direction of the neutron wave vector transfer  $\mathbf{Q} = \mathbf{k}_f - \mathbf{k}_i$  with respect to the wafer plane. The square outline indicates the size of the neutron beam incident on the sample.

to the lipid head group in reasonable agreement with values inferred from NMR measurements [5] and molecular-dynamics (MD) simulations [13].

We have now been able to fabricate samples of single-supported bilayer membranes of the *anionic* lipid DMPG (1,2-Dimyristoyl-*sn*-glycero-3-phosphoglycerol) that are large enough for QENS measurements and with a quality comparable to the DMPC samples. The DMPG and DMPC molecules both contain two aliphatic chains of 14 carbons. They differ only in the terminal subunit of their head group: the positively charged choline terminus in DMPC is replaced by a neutral glycerol in DMPG. Thus, we have the possibility of studying the effect of this single change in the head group structure on the mobility of the hydration water.

Like DMPC, we find that a similarly supported anionic DMPG bilayer shows evidence of bulk-like and confined water. However, the temperature dependence of the incoherent elastically scattered neutron intensity reveals a qualitative difference between the two membranes in the freezing and melting transitions of both types of associated water. To our knowledge, this

disparity in the freezing/melting behavior and the concomitant water dynamics in proximity to supported PC and PG membranes have not been observed heretofore. Because these model membrane systems are amenable to molecular-dynamics (MD) simulations, our results potentially offer sensitive tests of the electrostatic interactions and hydrogen bonding between water molecules and the lipid head groups.

As described previously, we deposited the single-supported DMPC membranes by a vesicle fusion process [12,14]. The substrate consisted of a cylindrical stack of about 100 acid-cleaned, electronic-grade Si(100) wafers (5 cm diameter, 0.3 mm thick, and polished on both sides) as shown in fig. 1(b) [15]. DMPC ( $\text{C}_{36}\text{H}_{72}\text{NO}_8\text{P}$ ) from Avanti Polar Lipids<sup>1</sup> was added to a solution of 100 mM KCl ( $M = \text{mol/L}$ ), 5 mM  $\text{MgCl}_2$ , and 2 mM HEPES ( $\text{C}_8\text{H}_{18}\text{N}_2\text{O}_4\text{S}$ ) and sonicated at 45 °C for ~24 h to produce multilamellar vesicles of micron size as confirmed by dynamic light scattering. After deposition of the DMPC, the wafers were rinsed in distilled water to remove additional membrane layers and dried in  $\text{N}_2$  gas. The wafer stack was loaded into an aluminum cell sealed with an indium O-ring under an argon atmosphere. Although not precisely controlled, the hydration level of the membranes could be varied by first annealing the samples in an oven at 328 K prior to loading them in the aluminum cell and then rehydrating them by introducing a water droplet into the sample can before sealing.

We have found deposition by vesicle fusion of large, homogeneous, single-supported DMPG ( $\text{C}_{34}\text{H}_{66}\text{O}_{10}\text{P}$ ) membranes to be more difficult than for DMPC. Previous atomic force microscopy (AFM) studies of PG membranes have used smaller samples of POPG (1-palmitoyl-2-oleoyl-*sn*-glycero-3-phosphoglycerol) deposited on a mica substrate by a Langmuir-Blodgett technique [16]. Our preparation of the sodium salt of DMPG as provided by Avanti Polar Lipids (see footnote <sup>1</sup>) began by obtaining the dry lipid powder by evaporation under nitrogen gas from a 65:35:8 chloroform:methanol:water solution. We then rehydrated the powder solution of 15 mM KCl and 15 mM  $\text{MgCl}_2$ . A higher concentration of  $\text{MgCl}_2$  than for the deposition of single membranes of DMPC was required to facilitate formation of planar membrane structures. The solution was heated to 70 °C and sonicated for ~1 h to break up larger aggregates before filtering through a 100 nm filter in a Liposofast apparatus also from Avanti (see footnote <sup>1</sup>). The resultant solution was clear and contained small, mostly unilamellar vesicles.

The DMPG was then diluted to a concentration of 15  $\mu\text{g/ml}$ . Silicon wafers were immersed in the solution and incubated for 1 h at 65 °C during which time the

<sup>1</sup>Certain commercial equipment, instruments, or materials (or suppliers) are identified in this paper to foster understanding. Such identification does not imply recommendation or endorsement by the National Institute of Standards and Technology, nor does it imply that the materials or equipment identified are necessarily the best available for this purpose.

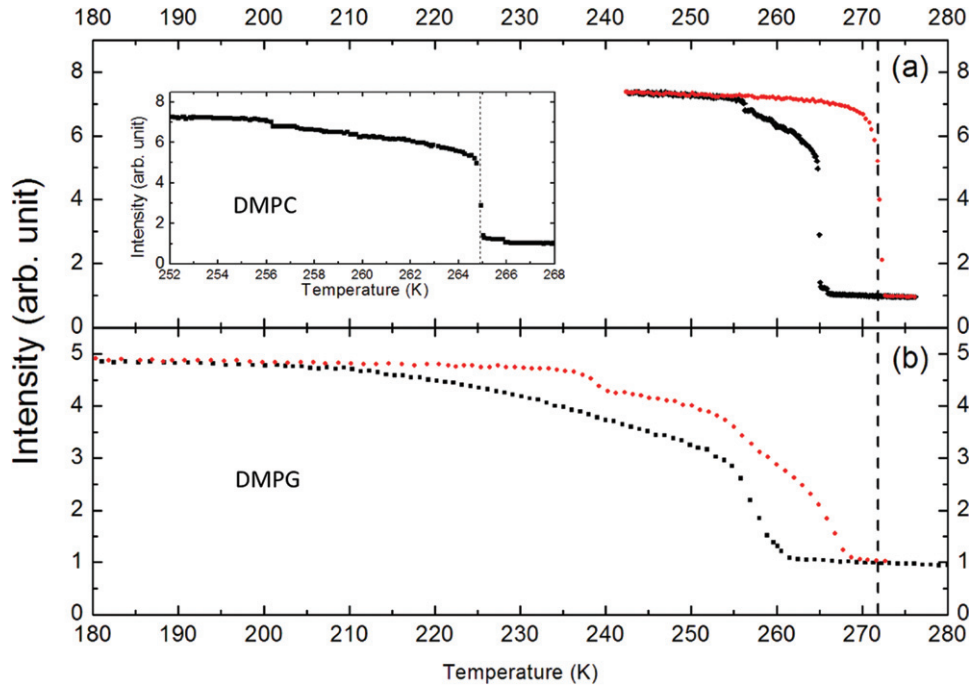


Fig. 2: (Color online) Comparison of the elastic intensity measured on the backscattering spectrometer HFBS at NIST as a function of temperature in a cooling/heating cycle for well-hydrated single-supported membranes: (a) DMPC; and (b) DMPG. Data taken on cooling are shown by squares (black) and on heating by circles (red). The data for DMPC in (a) are from ref. [12].

vesicle fusion occurred. Upon removal, water appeared to wet to the wafer, in contrast to wafers with deposited DMPC, and the remaining buffer solution was allowed to evaporate in air.

Topographic images recorded by AFM from similarly prepared samples under a flow of moist air showed homogeneous DMPC and DMPG membranes of comparable quality with few holes or cracks [17,18]. The membranes had a typical thickness of  $\sim 6.3$  nm at room temperature, which is somewhat larger than the  $\sim 4.6$  nm reported from neutron reflectivity measurements on single-supported DMPC membranes submerged in  $D_2O$  [19]. Possible reasons for this discrepancy have been discussed in ref. [12]. The temperature dependence of the membrane thickness measured by AFM indicated that below 328 K both the DMPC and DMPG bilayers were in their gel phase [17,18].

In fig. 2(a), we show the temperature dependence of the intensity of incoherent elastically scattered neutrons from a sample of single-supported DMPC membranes [12] as measured on the High-Flux Backscattering Spectrometer (HFBS) at the NIST (National Institute of Standards and Technology) Center for Neutron Research [20]. This so-called wet sample was prepared by first annealing in air for 72 h at a temperature of 328 K before sealing the wafer stack in the sample can with  $120 \mu\text{l}$  of  $H_2O$  to ensure an excess of water above the membranes (see below). The elastic intensity was recorded on both slow cooling of the sample ( $0.04$  K/min, black points) and on heating ( $0.1$  K/min, red points). It has been summed over all wave

vector transfers to increase the intensity and measures the number of neutrons scattered with energy transfers less than  $\sim 1 \mu\text{eV}$ , the full width at half-maximum (FWHM) of the HFBS' resolution function. Because incoherent scattering from the hydrogen atoms dominates the elastic signal, a decrease in elastic intensity is proportional to an increase in the number of H atoms in the sample moving on a time scale faster than  $\sim 1$  ns. As discussed in ref. [12], most of the H atoms in this wet sample are in the  $H_2O$  molecules so that at low temperatures water provides the dominant contribution to the elastic intensity. At temperatures above 273 K, where the elastic intensity levels off at its lowest value, the motion of H atoms in both water and membrane are faster than the time scale of the instrument so that all of the elastic scattering is contributed by the silicon substrate.

Because the silicon substrate is identical to that used previously in our study of alkane films [15], we can use the increase in elastic intensity measured on cooling of alkane films of known coverage to estimate the number of H atoms in our membrane samples [12]. Allowing for the H atoms in the single membrane bilayer coating each side of the 100 silicon wafers, we can calculate the remaining number of H atoms associated with the water in the samples.

Assuming the water to have its bulk density, we estimate that the wet DMPC sample in fig. 2(a) contains an amount of water equivalent to a slab  $\sim 100$  nm thick on each side of a wafer. However, we emphasize that the morphology of the water is unknown [12]. That is, some

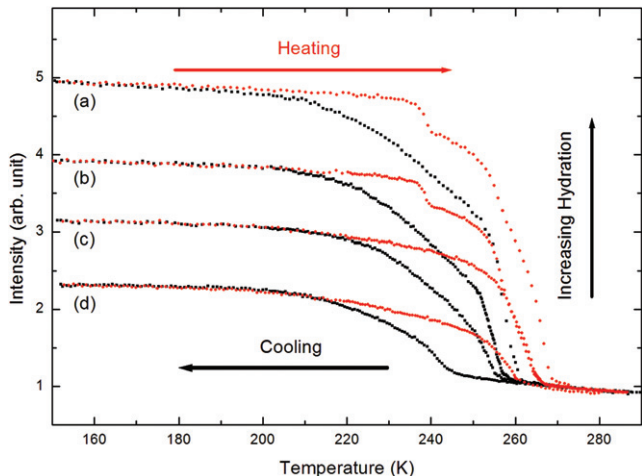


Fig. 3: (Color online) Elastic scans measured on the HFBS for DMPG samples having four different levels of hydration. The corresponding water thicknesses (see text) are: 71 nm (a); 52 nm (b); 39 nm (c); and 23 nm (d). The scans labeled (a) are the same as those in fig. 2(b).

of the water could be in the form of droplets rather than in a slab of uniform thickness.

In fig. 2(b), we see that a wet DMPG membrane exhibits a temperature dependence of the elastic intensity that differs qualitatively from that of the wet DMPC sample both on cooling and heating (fig. 2(a)). The wet DMPC sample shows a vertical step in the elastic intensity on cooling to a temperature of 265 K followed by a continuous increase in intensity whereas the DMPG membrane displays only a continuous increase in the elastic intensity below  $\sim 270$  K. The rate of increase of the elastic intensity for the DMPG sample exhibits three distinct temperature ranges: an initial rapid rise ( $255 \text{ K} < T < 260 \text{ K}$ ); a range of reduced slope ( $230 \text{ K} < T < 250 \text{ K}$ ); and a range over which the intensity levels off ( $T < 230 \text{ K}$ ). The elastic intensity does not reach its low-temperature limit until  $\sim 200$  K or about 50 K lower than for DMPC. We do not believe the different freezing behavior of the DMPG sample can be attributed to its lower hydration level (equivalent water thickness  $\sim 71$  nm) because another DMPC sample (equivalent water thickness of  $\sim 83$  nm) showed qualitatively similar freezing behavior to that of the wet sample in fig. 2(a) [18].

On heating, the temperature dependence of the elastic intensity again differs for the two membranes. We see (fig. 2(b)) that the DMPG membrane has a downward substep near 240 K followed by weaker substeps near 255 K and 264 K, respectively, with the intensity leveling off at 270 K; *i.e.*, below the melting point of bulk ice. In contrast, the elastic intensity measured on the DMPC membrane shows a single abrupt step at the melting point of bulk ice, 273 K.

In fig. 3, we show elastic scans taken on the HFBS from four single-supported DMPG membrane samples having different levels of hydration. The equivalent water

thickness of these samples ranged from  $\sim 23$  nm to  $\sim 71$  nm. All of the samples exhibit a qualitatively similar and highly reproducible behavior on cooling, differing principally in the onset temperature of the increase in elastic intensity and the magnitude of its initial rise. On heating, however, the two samples having the lowest hydration level do not show the step-like decreases in intensity as seen at higher hydration. For all of the DMPG samples, the intensity reaches its minimum value corresponding to the elastic scattering from the silicon substrate at a temperature below the melting point of bulk ice at 273 K.

The contrasting temperature dependence of the elastic scans for the DMPC and DMPG membranes shown in fig. 2 suggests qualitative differences in the freezing/melting behavior of the membrane-associated water. We previously interpreted the step-like increase in the elastic intensity at  $\sim 265$  K on cooling the DMPC membrane as indicating the freezing of super-cooled bulk-like water above the lipid head groups [12]. This interpretation was supported by a heating curve showing a single step-like decrease in the elastic intensity at the bulk melting point of 273 K. The gradual increase in intensity on cooling down to 255 K was attributed to continuous freezing of confined water nearer the lipid head groups [12].

Similarly, we interpret the continuous increase of the elastic intensity on cooling the DMPG sample to  $\sim 200$  K as indicating a continuous freezing of water, a transition that extends over a much larger temperature range than for DMPC. Although the initial, steep rise in intensity is not as abrupt as for DMPC, the fact that the intensity increment in this temperature range scales with the total amount of water in the sample (see fig. 3) suggests that, like DMPC, it is due to the freezing of bulk-like water above the membrane. At lower temperatures ( $T < 250$  K), the intensity increment on cooling the DMPG sample is relatively insensitive to the total hydration. Therefore, we attribute it to the freezing of confined water closer to the lipid head groups that is present in roughly the same amount in all of the samples. We suggest that the inflection in the temperature dependence of the elastic intensity near  $\sim 230$  K present for the three DMPG samples of highest hydration in fig. 3 may indicate a freezing transition of a portion of the confined water, leaving a second component of confined water mobile.

We are uncertain as to why, unlike DMPC, all of the water associated with the DMPG membrane melts continuously below the bulk melting point of 273 K. The solid water might be confined in such a way as to reduce its melting point, or it might be amorphous. Neutron diffraction experiments are now underway to search for evidence of polycrystalline ice in both the DMPC and DMPG samples [21]. Also, we are uncertain of the origin of the substeps observed in the elastic intensity on heating the two DMPG samples having the highest level of hydration. Possibly they arise from successive melting transitions corresponding to the freezing transitions of two types of confined water tentatively identified on cooling

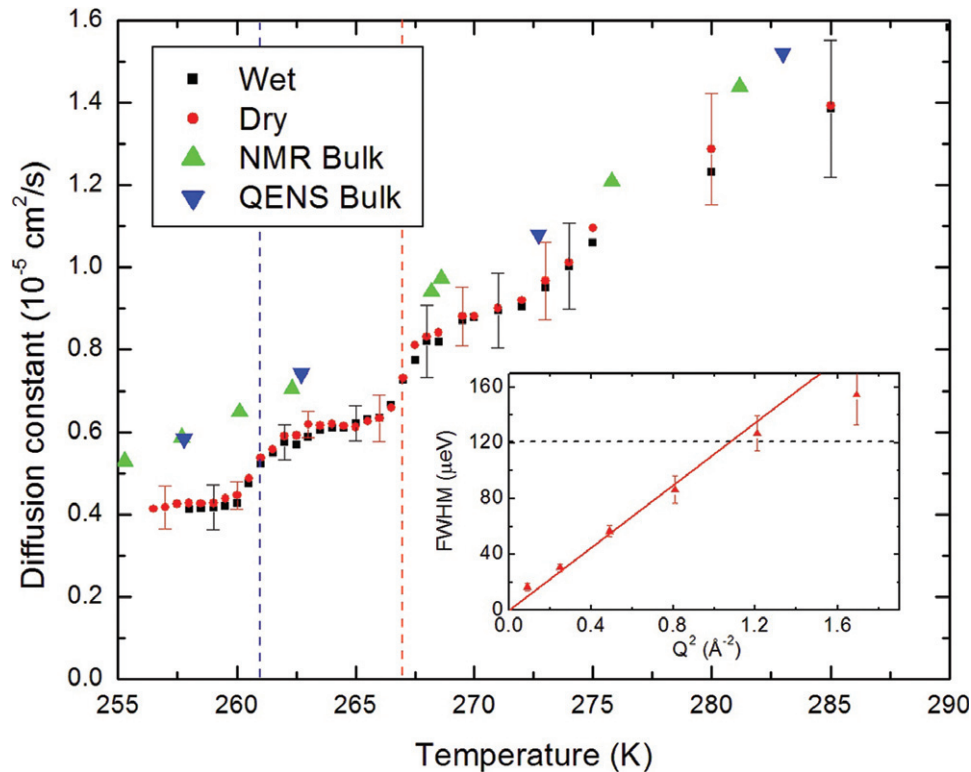


Fig. 4: (Color online) Diffusion constant  $D$  vs. temperature for wet and dry samples of DMPC (see text). The green up (blue down) triangles are values for bulk water from NMR (QENS) measurements.  $D$  is half the slope of the line fit to the low- $Q$  points in the plot of the FWHM of the QENS vs.  $Q^2$  as shown in the inset. The data in the inset were taken at a temperature of 270 K. Error bars represent one standard deviation. The horizontal dashed line in the inset indicates approximately the useful dynamic range of BASIS.

followed by continuous melting of the bulk-like water at higher temperature.

To investigate the dynamics of the bulk-like and confined water proposed from our temperature scans of elastic neutron intensity, we have also obtained full quasielastic spectra from our DMPC sample and used them to determine the diffusion constant of the water throughout its freezing transition. The measurements were performed on the backscattering spectrometer BASIS at the Spallation Neutron Source, Oak Ridge National Laboratory [22]. On cooling the wet sample in fig. 2(a), we obtained spectra with a counting time of 1 h at a temperature interval of 0.5 K [12]. We fit the spectra by folding the instrumental resolution function with a scattering law composed of three terms: a delta function corresponding to the elastic scattering plus two Lorentzians representing the quasielastic scattering. The decomposition of a spectrum into these three components and a linear background term is illustrated in fig. 3 of ref. [12]. The temperature dependence of the delta-function intensity agrees well with that of the elastic intensity measured on the HFBS as shown in fig. 2(a) except that the step-like increase in intensity on cooling occurred about three degrees higher at 268 K. Similar measurements of the QENS spectra from our DMPC samples are now in progress.

The large dynamic range of BASIS allowed us to resolve two diffusive processes occurring at different rates: a “fast” motion (time scale  $< 40$  ps) that can be fit to a broad Lorentzian (dotted (green) curve) and a “slow” motion (time scale  $\sim 0.5$  ns) described by a narrow Lorentzian (dashed (red) curve) (see fig. 3 in ref. [12]). The FWHM of the broad Lorentzian has a  $Q^2$ -dependence at low  $Q$  as shown in the inset to fig. 4 characteristic of translational diffusion. Measurements with this wet sample at a temperature of 275 K yielded a diffusion constant  $D$  of  $1.02 \times 10^{-5} \text{ cm}^2/\text{s}$  close to but smaller than the value of  $1.13 \times 10^{-5} \text{ cm}^2/\text{s}$  obtained previously for bulk water at this temperature [23,24]. Therefore, above the step-like increase in the elastic intensity at 268 K (see fig. 2(a)), we identified the broad Lorentzian component with translational diffusion in “bulk-like” water [12]. Here we use the term “bulk-like” to indicate a diffusion constant close to but somewhat smaller than the bulk value as determined by NMR and QENS measurements in this temperature range. The narrow Lorentzian, whose width was nearly  $Q$ -independent, was identified with the diffusive motion of H atoms within the lipid molecules and the water bound to their head groups [12].

In fig. 4, we plot  $D$  for both the wet DMPC sample of fig. 2(a) and a “dry” sample [12] below room temperature.

Despite having about a factor of six less water, the dry sample (water thickness  $\sim 17$  nm) has nearly the same value of  $D$  as the wet sample over the entire temperature range. Apparently, the amount of water above the membrane in the dry sample is large enough to result in bulk-like diffusion above 265 K. At the abrupt freezing transition of the bulk-like water at 265 K (see inset to fig. 2(a)), there is step-like decrease in  $D$  to a value of  $0.61 \times 10^{-5} \text{ cm}^2/\text{s}$  that we interpret to be that of confined water. On further cooling, there is a temperature range where  $D$  remains nearly constant at this value ( $262 \text{ K} < T < 266 \text{ K}$ ) before another step-like decrease in  $D$  occurs at  $\sim 261 \text{ K}$  to a value of  $0.41 \times 10^{-5} \text{ cm}^2/\text{s}$ . This behavior, consistent with a freezing of one type of confined water with a second type still diffusing at lower temperatures, as we have suggested might be occurring in the DMPG sample. However, unlike the freezing transition of the bulk-like water, it is more difficult to discern a corresponding step-like increase in the elastic intensity at  $\sim 261 \text{ K}$  (see inset to fig. 2(a) above and figs. 4(a) and (d) in ref. [12]). While this interpretation is speculative, it is clear that similar step-like decreases in the temperature dependence of  $D$  for the wet and dry DMPC samples differ qualitatively from the relatively smooth dependence of bulk supercooled water as determined by NMR [24] and QENS [23] measurements.

In summary, incoherent elastic and quasielastic neutron scattering reveal the sensitivity of the freezing transition and dynamics of the interfacial water to the charge state of the lipid head groups in these model membrane systems. While we have found evidence of bulk-like and two types of confined water common to both the zwitterionic and anionic membranes, the width and character of the freezing transition of the two membranes differ greatly. Our measurements motivate detailed MD simulations of these model membranes to elucidate the electrostatic interactions and hydrogen bonding of the interfacial water. For example, knowledge of these interactions may shed light on why the freezing of the hydration water for DMPG is greatly depressed compared to that of DMPC. We also plan to search for evidence of water bound to the head groups as we have found for the DMPC membrane.

\*\*\*

This work was supported by the U.S. National Science Foundation under Grant Nos. DMR-0705974 and DGE-1069091 and utilized facilities supported in part by the NSF under agreement No. DMR-0454672. A portion of this research at Oak Ridge National Laboratory's Spallation Neutron Source was sponsored by the Scientific User Facilities Division, Office of Basic Energy Sciences, U.S. Department of Energy. We thank DAN A. NEUMANN and IOAN KOSZTIN for helpful discussions.

## REFERENCES

- [1] SALSBUURY N. J., DARKE A. and CHAPMAN D., *Chem. Phys. Lipids*, **8** (1972) 142.
- [2] FINER E. G., *J. Chem. Soc., Faraday Trans.*, **69** (1973) 1590.
- [3] BAYERL T. M. and BLOOM M., *Biophys. J.*, **58** (1990) 357.
- [4] KÖNIG S., SACKMANN E., RICHTER D., ZORN R., CARLILE C. and BAYERL T. M., *J. Chem. Phys.*, **100** (1994) 3307.
- [5] FAURE C., BONAKDAR L. and DUFOURC E. J., *FEBS Lett.*, **405** (1997) 263.
- [6] KAUSIK R. and HAN S., *Phys. Chem. Chem. Phys.*, **13** (2011) 7732.
- [7] PFEIFFER W., HENKEL TH., SACKMANN E., KNOLL W. and RICHTER D., *Europhys. Lett.*, **8** (1989) 201.
- [8] KÖNIG S., PFEIFFER W., BAYERL T., RICHTER D. and SACKMANN E., *J. Phys. II*, **2** (1992) 1589.
- [9] RHEINSTÄDTER M. C., SEYDEL T., DEMMEL F. and SALDITT T., *Phys. Rev. E*, **71** (2005) 061908.
- [10] SWENSON J., KARGI F., BERNSTEN P. and SVANBERG C., *J. Chem. Phys.*, **129** (2008) 045101.
- [11] TRAPP M., GUTBERLET T., JURANYI F., UNRUH T., DEMÉ B., TEHEI M. and PETERS J., *J. Chem. Phys.*, **133** (2010) 164505.
- [12] BAI M., MISKOWIEC A., HANSEN F. Y., TAUB H., JENKINS T., TYAGI M., DIALLO S. O., MAMONTOV E., HERWIG K. W. and WANG S.-K., *EPL*, **98** (2012) 48006.
- [13] HANSEN F. Y., PETERS G. H., TAUB H. and MISKOWIEC A., *J. Chem. Phys.*, **137** (2012) 204919.
- [14] CASTELLANA E. T. and CREMER P. S., *Surf. Sci. Rep.*, **61** (2006) 429.
- [15] WANG S.-K., MAMONTOV E., BAI M., HANSEN F. Y., TAUB H., COPLEY J. R. D., GARCÍA SAKAI V., GASPAROVIC G., JENKINS T., TYAGI M., HERWIG K. W., NEUMANN D., MONTFROOIJ W. and VOLKMANN U. G., *EPL*, **91** (2010) 66007.
- [16] PICAS L., SUÁREZ-GERMÀ C., MONTERO M. T. and HERNÁNDEZ-BORRELL J., *J. Phys. Chem. B*, **114** (2010) 3543.
- [17] MISKOWIEC A., BUCK Z. N., SCHNASE P., KAISER H., HEITMANN T., MICELI P. F., BAI M., TAUB H., HANSEN F. Y., KING G. M., DUBEY M., SINGH S. and MAJEWSKI J., unpublished.
- [18] JOHNSON S. J., BAYERL T. M., MCDERMOTT D. C., ADAM G. W., RENNIE A. R., THOMAS R. K. and SACKMANN E., *Biophys. J.*, **59** (1991) 289.
- [19] MAYER A., DIMEO R., GEHRING P. and NEUMANN D., *Rev. Sci. Instrum.*, **74** (2003) 2759.
- [20] MISKOWIEC A., PhD Thesis, University of Missouri, 2014 (unpublished).
- [21] BUCK Z. N., MISKOWIEC A., KAISER H., HANSEN F. Y. and TAUB H., unpublished.
- [22] MAMONTOV E. and HERWIG K. W., *Rev. Sci. Instrum.*, **82** (2011) 085109.
- [23] TEIXEIRA J., BELLISSENT-FUNEL M.-C., CHEN S. H. and DIANOUX A. J., *Phys. Rev. A*, **31** (1985) 1913.
- [24] PRICE W. S., IDE H. and ARATA Y., *J. Phys. Chem. A*, **103** (1999) 448.